

Journal club: quantum dot entropy measurement

07.03.2025

Two related papers

2018

Direct entropy measurement in a mesoscopic quantum system

Nikolaus Hartman^{1,2*}, Christian Olsen^{1,2}, Silvia Lüscher^{1,2}, Mohammad Samani^{1,2,3,9}, Saeed Fallahi^{4,5,6}, Geoffrey C. Gardner^{5,6,7}, Michael Manfra^{4,5,6,7,8} and Joshua Folk^{1,2*}

The entropy of an electronic system offers important insights into the nature of its quantum mechanical ground state. This is particularly valuable in cases where the state is difficult to identify by conventional experimental probes, such as conductance. Traditionally, entropy measurements are based on bulk properties, such as heat capacity, that are easily observed in macroscopic samples but are unmeasurably small in systems that consist of only a few particles^{1,2}. Here, we develop a mesoscopic circuit to directly measure the entropy of just a few electrons, and demonstrate its efficacy using the well-understood spin statistics of the first, second and third electron ground states in a GaAs quantum dot³⁻⁸. The precision of this technique, quantifying the entropy of a single spin-1/2 to within 5% of the expected value of $k_B \ln 2$, shows its potential for probing more exotic systems. For example, entangled states or those with non-Abelian statistics could be clearly distinguished by their low-temperature entropy⁹⁻¹³.

2022

Entropy Measurement of a Strongly Coupled Quantum Dot

Timothy Child^{1,2,*}, Owen Sheekey^{1,2}, Silvia Lüscher^{1,2}, Saeed Fallahi^{3,4}, Geoffrey C. Gardner^{4,5}, Michael Manfra^{3,4,6,5}, Andrew Mitchell^{7,8}, Eran Sela⁹, Yaakov Kleeorin¹⁰, Yigal Meir^{11,12} and Joshua Folk^{1,2,†}

¹Stewart Blusson Quantum Matter Institute, University of British Columbia, Vancouver, British Columbia, V6T1Z4, Canada

²Department of Physics and Astronomy, University of British Columbia, Vancouver, British Columbia, V6T1Z1, Canada

³Department of Physics and Astronomy, Purdue University, West Lafayette, Indiana 47907, USA

⁴Birck Nanotechnology Center, Purdue University, West Lafayette, Indiana 47907, USA

⁵School of Materials Engineering, Purdue University, West Lafayette, Indiana 47907, USA

⁶Elmore Family School of Electrical and Computer Engineering, Purdue University, West Lafayette, Indiana 47907, USA

⁷School of Physics, University College Dublin, Belfield, Dublin 4, Ireland

⁸Centre for Quantum Engineering, Science, and Technology, University College Dublin, Dublin 4, Ireland

⁹Raymond and Beverly Sackler School of Physics and Astronomy, Tel-Aviv University, IL-69978 Tel Aviv, Israel

¹⁰Center for the Physics of Evolving Systems, University of Chicago, Chicago, Illinois 60637, USA

¹¹Department of Physics, Ben-Gurion University of the Negev, Beer Sheva 84105, Israel

¹²The Ilse Katz Institute for Nanoscale Science and Technology, Ben-Gurion University of the Negev, Beer Sheva 84105, Israel



(Received 27 April 2022; accepted 28 October 2022; published 22 November 2022)

The spin 1/2 entropy of electrons trapped in a quantum dot has previously been measured with great accuracy, but the protocol used for that measurement is valid only within a restrictive set of conditions. Here, we demonstrate a novel entropy measurement protocol that is universal for arbitrary mesoscopic circuits and apply this new approach to measure the entropy of a quantum dot hybridized with a reservoir. The experimental results match closely to numerical renormalization group (NRG) calculations for small and intermediate coupling. For the largest couplings investigated in this Letter, NRG calculations predict a suppression of spin entropy at the charge transition due to the formation of a Kondo singlet, but that suppression is not observed in the experiment.

Why measure entropy?

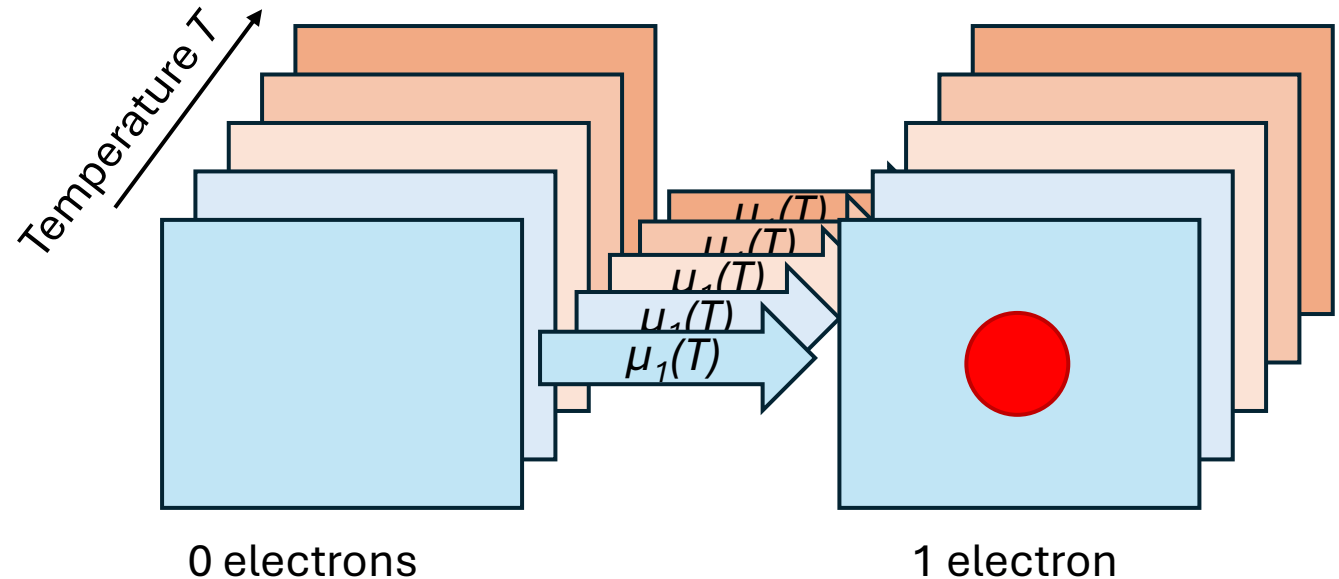
- Distinguish quantum states otherwise similar by their conductance for example
- Distinguish non-abelian quasi-particles from abelian ones
 - Challenging due to small signal size around k_B

Entropy-to-charge conversion in a ‘few-electron GaAs quantum dot’: Principle

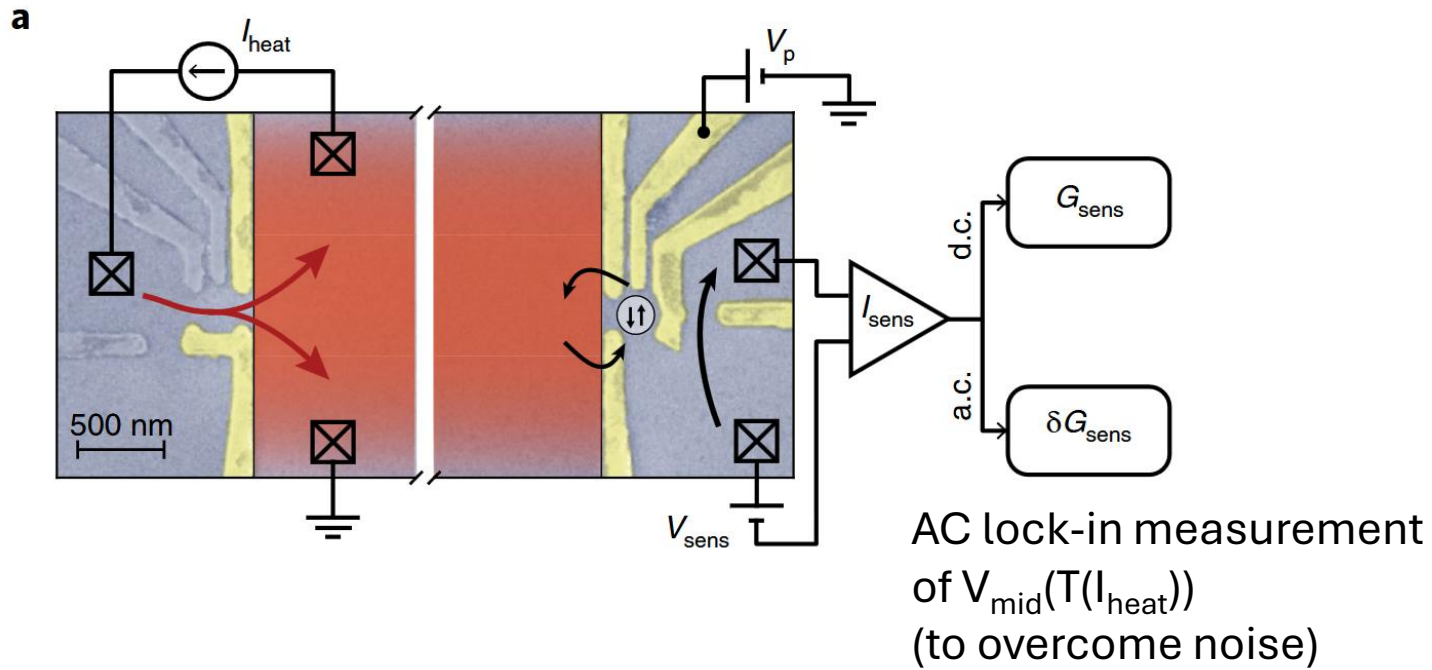
$$\left(\frac{\partial \mu}{\partial T} \right)_{p, N} = - \left(\frac{\partial S}{\partial N} \right)_{p, T}$$

Maxwell relation, where
 p : pressure
 N : particle number
 S : entropy
 T : temperature
 μ : chemical potential

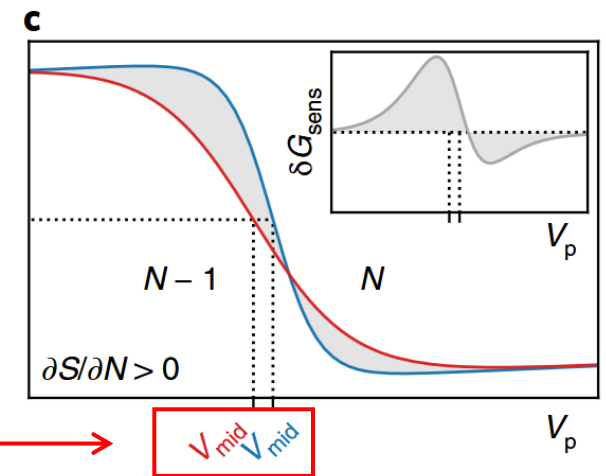
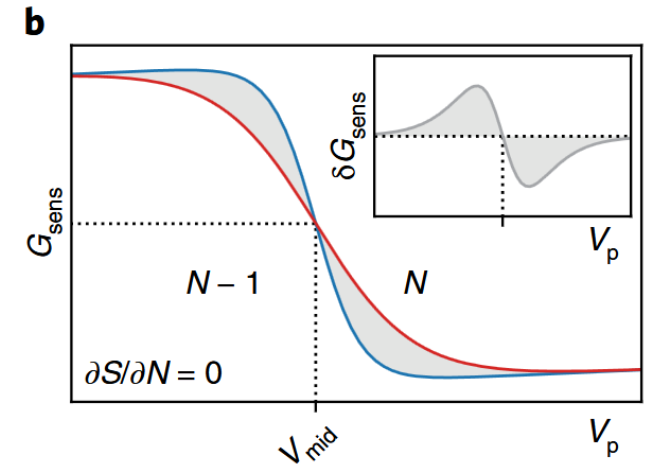
‘the entropy difference between the $N - 1$ and N electron ground states is measured via the shift with temperature in the electrochemical potential μ_N needed to add the N th electron to the dot’



Device operation



Charge sensor simulation



Shift in V_{mid} gives shift μ_N which gives S

Device operation details

$$G_{\text{sens}}(V_p, \Theta) = G_0 \tanh\left(\frac{V_p - V_{\text{mid}}(\Theta)}{2\Theta}\right) + \gamma_1 V_p + G_2$$

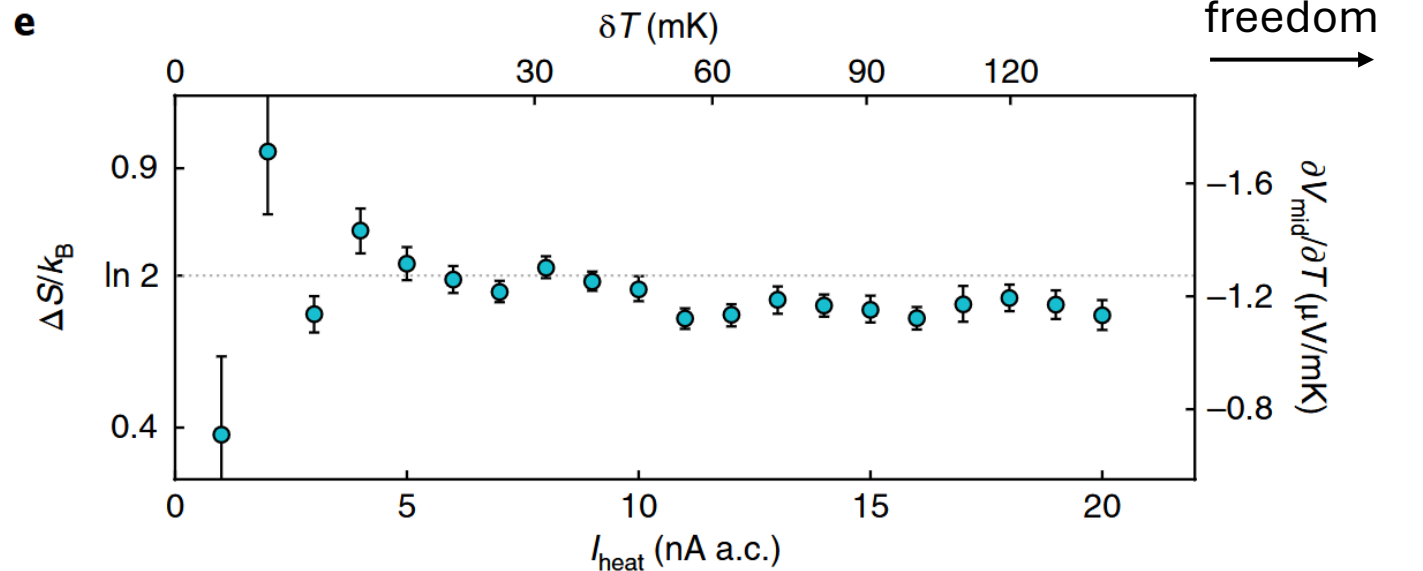
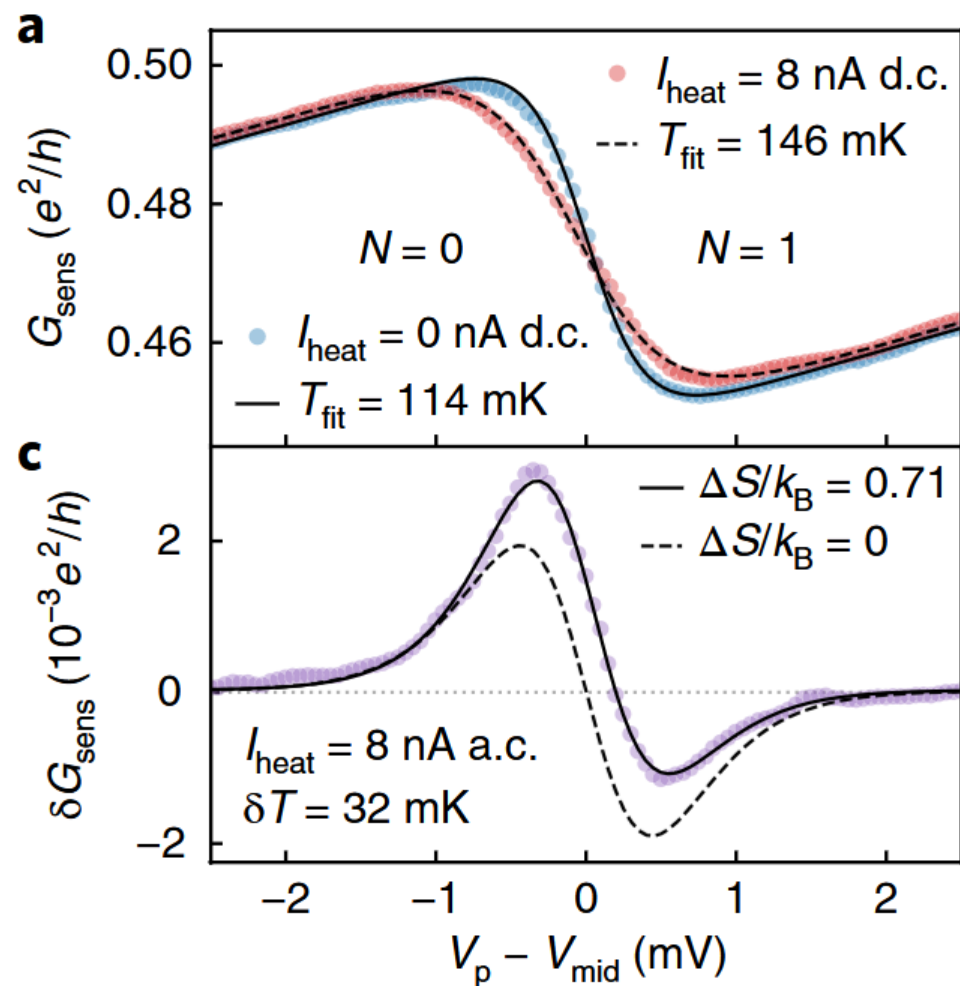
where G_0 quantifies the sensor sensitivity, $\Theta = \frac{k_B T}{\alpha e}$ is the thermal broadening expressed in units of gate voltage, $\alpha = \frac{1}{e} \frac{d\mu_N}{dV_p}$ is the lever arm, γ_1 reflects the cross-capacitance between the charge sensor and plunger gate, and G_2 is an offset

$$\frac{\partial V_{\text{mid}}}{\partial \Theta} = \frac{1}{k_B} \frac{\partial \mu}{\partial T} = -\frac{1}{k_B} \Delta S_{N-1 \rightarrow N}$$

$$\delta G_{\text{sens}}(V_p, \Theta) \propto -\delta T \left[\frac{V_p - V_{\text{mid}}(\Theta)}{2\Theta} - \frac{\Delta S}{2k_B} \right] \cosh^{-2}\left(\frac{V_p - V_{\text{mid}}(\Theta)}{2\Theta}\right)$$

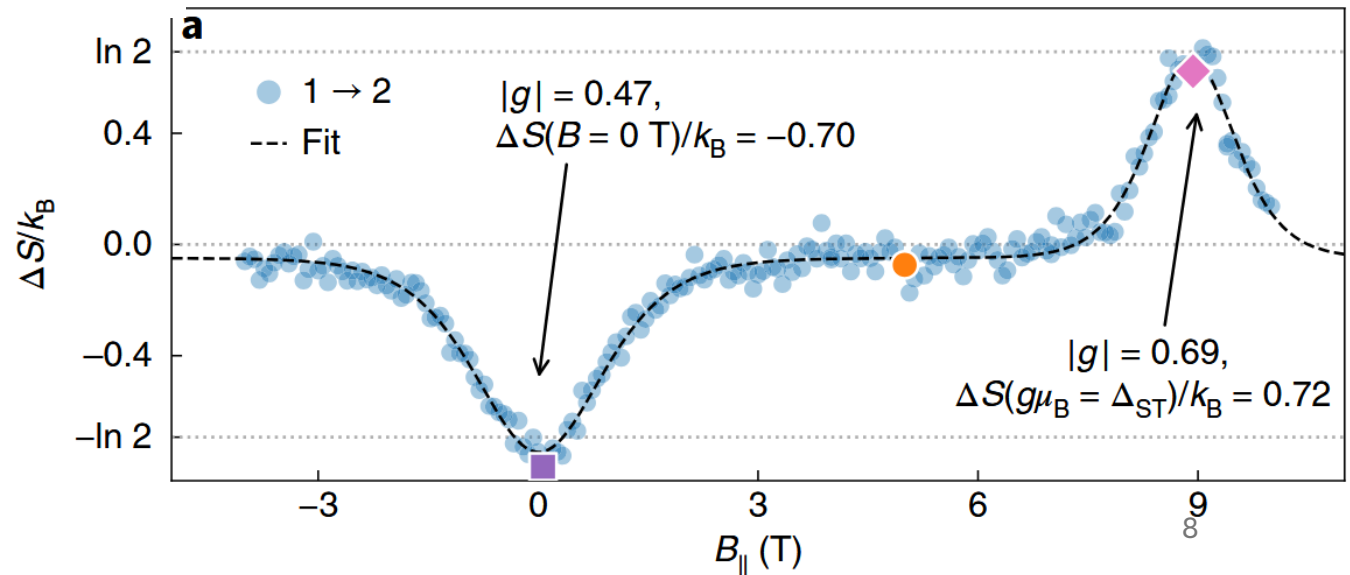
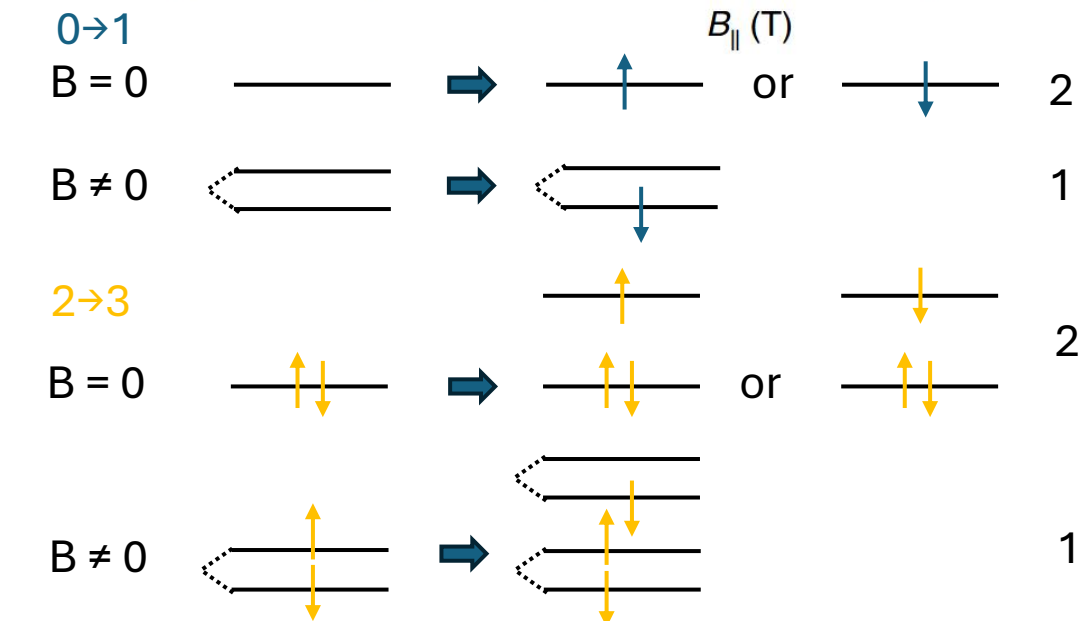
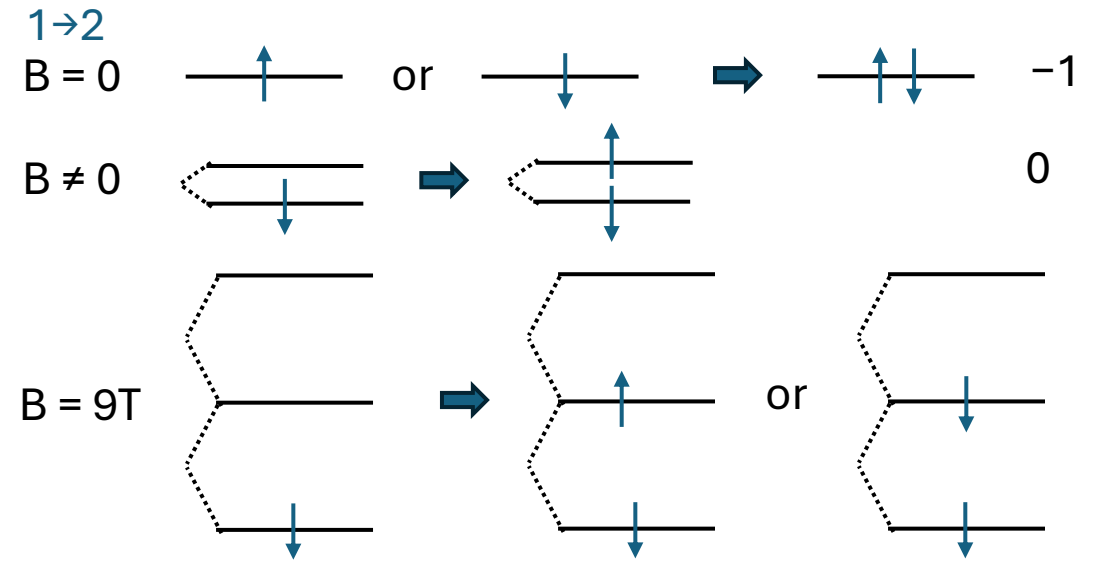
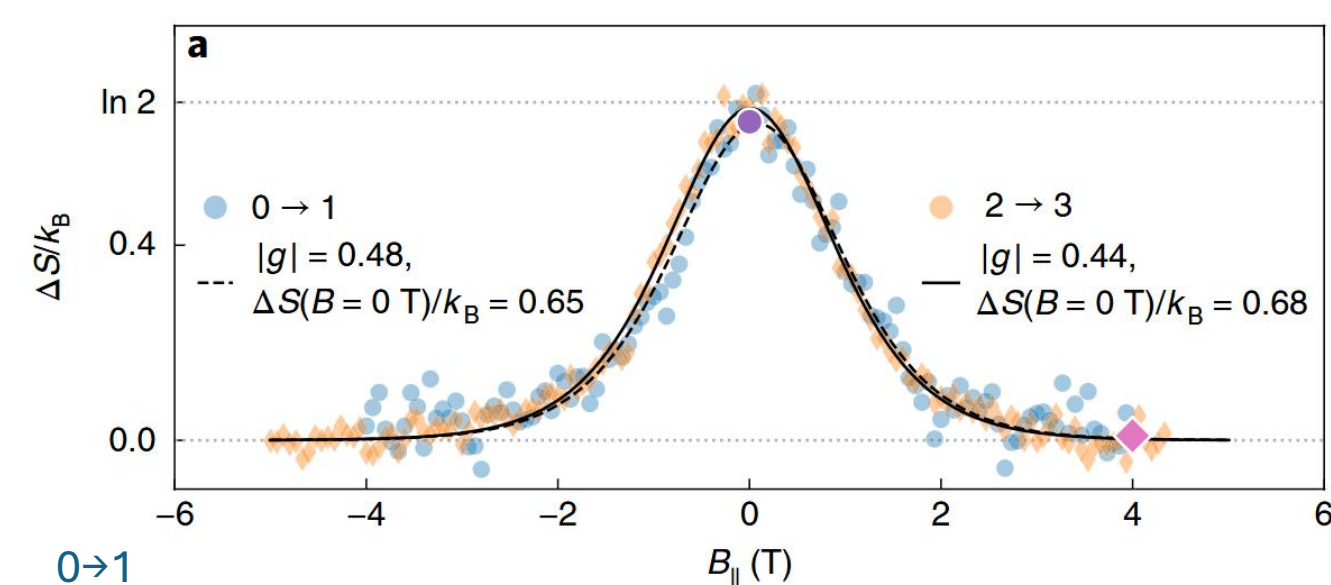
+ const.

Results



$\Delta S_{0 \rightarrow 1} = (1.02 \pm 0.03)k_B \ln 2$, closely matching the expected $\Delta S_{0 \rightarrow 1} = S_1 - S_0 = k_B \ln 2$ for transitions between an empty dot with zero entropy ($S_0 = 0$) and the two-fold degenerate one-electron state ($d_1 = 2$) with entropy $S_1 = k_B \ln 2$.

Results



More general entropy extraction method

$$d\Phi = -SdT - (N_{res} + N)d\mu + Nd\epsilon + \dots$$

↑
Grand potential

↑
Average occupation of reservoir

↙ ↘
QD occupation

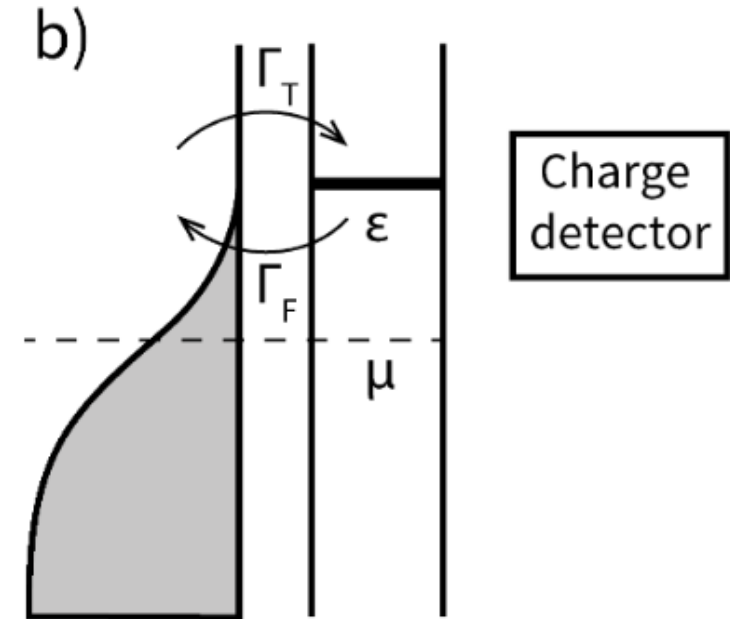
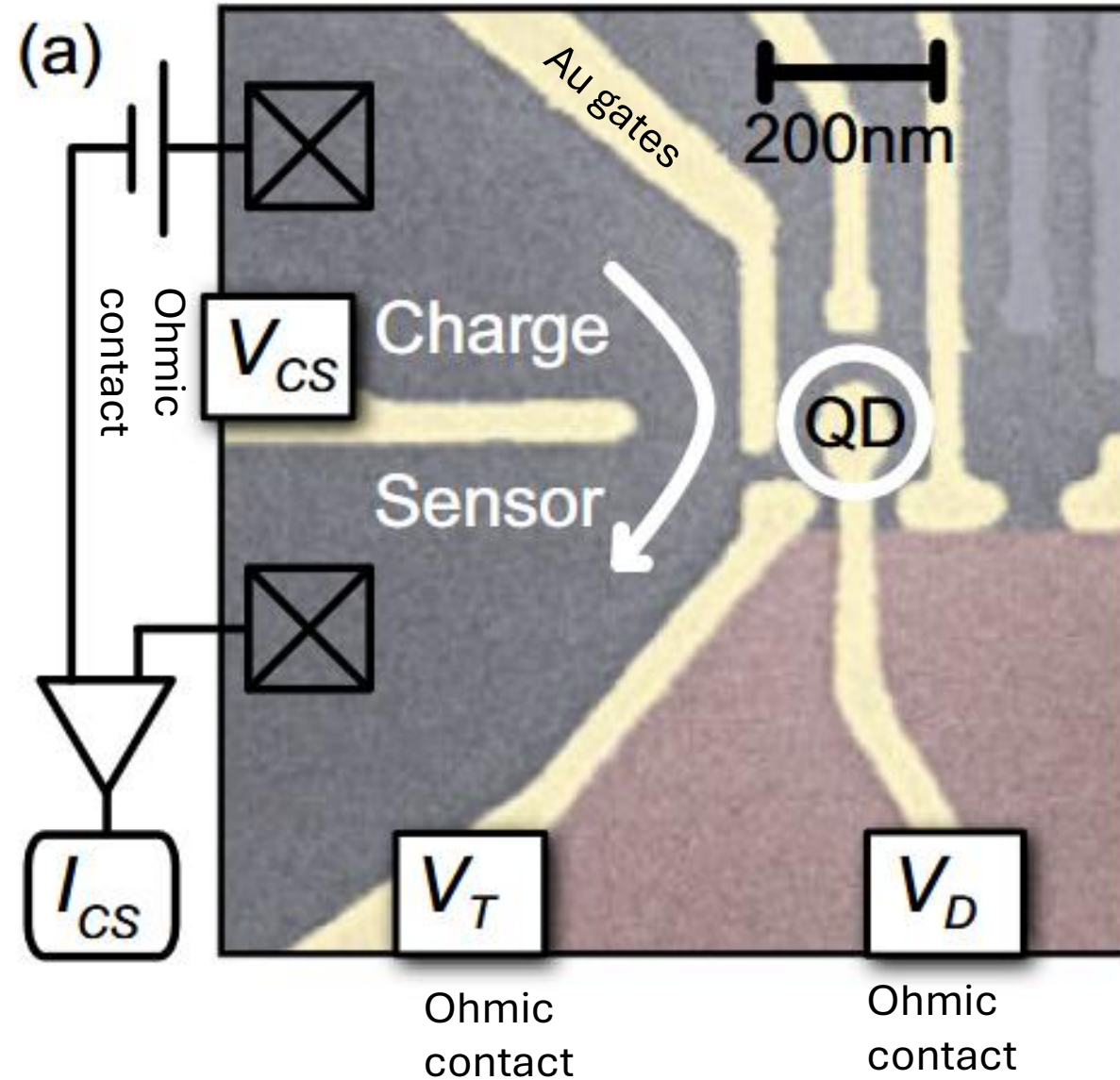
↑
Local potential for N , or gate-tuned QD energy

gives $\partial\Phi/\partial T = -S$ and $\partial\Phi/\partial\epsilon = N$ (Assumes that the hamiltonian has a term $H_{gate} = \epsilon\hat{N}$)

therefore $\partial N/\partial T = -\partial S/\partial\epsilon$

and finally $\Delta S_{\epsilon_1 \rightarrow \epsilon_2} = - \int_{\epsilon_1}^{\epsilon_2} \frac{dN(\epsilon)}{dT} d\epsilon$

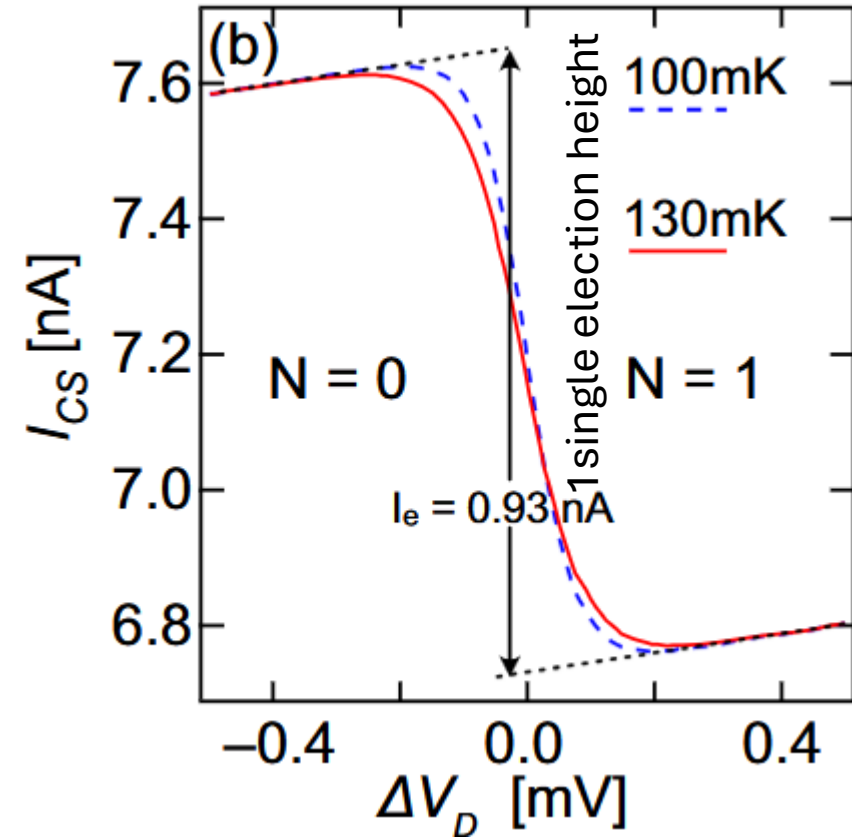
Device



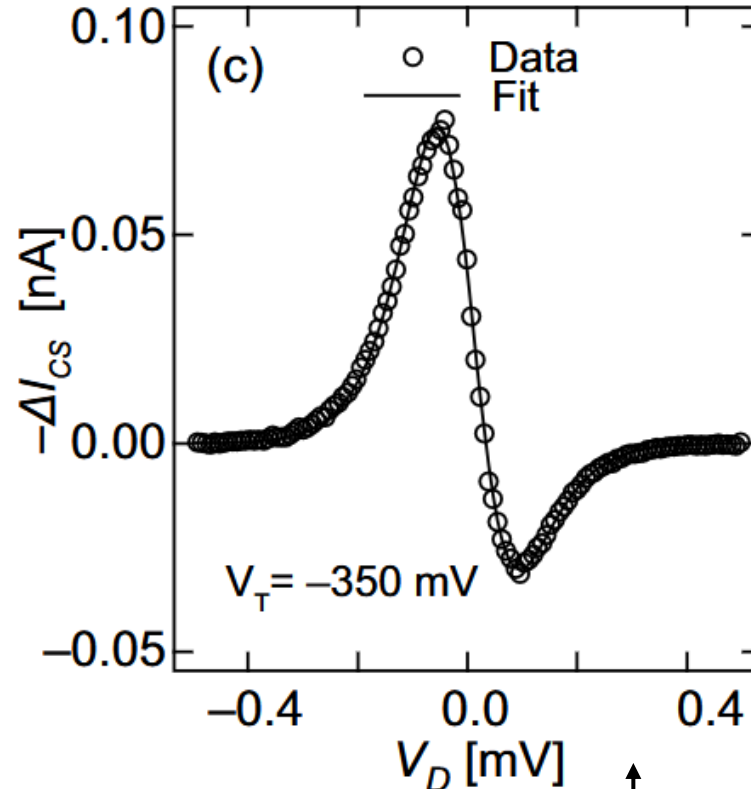
From Eugenia Pyurbeeva and Jan A. Mol, A thermodynamic approach to measuring entropy in a few-electron nano-device, Entropy 23, 640 (2021)

Charge sensor characterisation

0 to 1 transition in weakly coupled regime



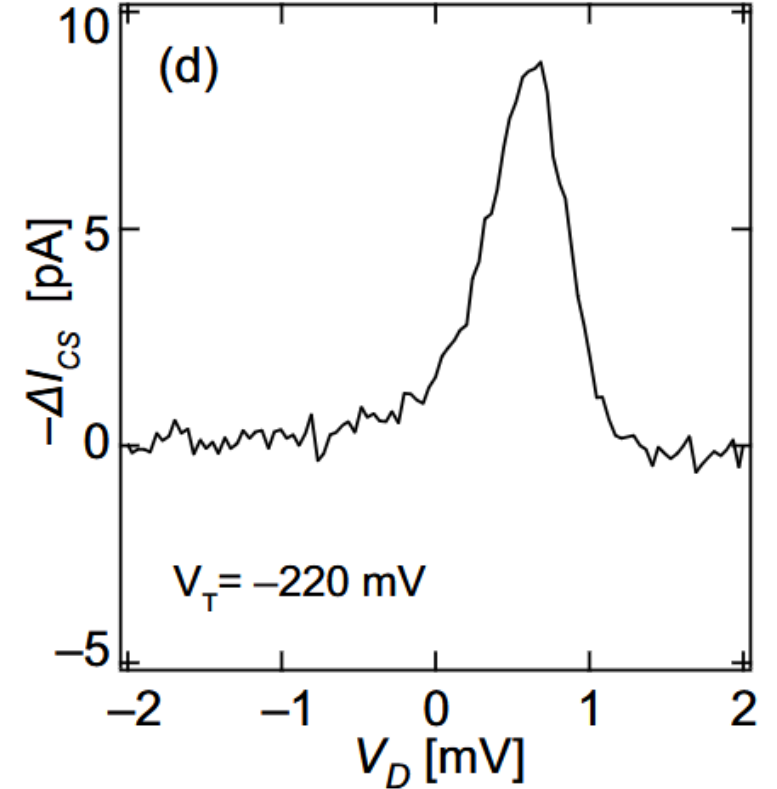
Weak coupling to reservoir
 $\Gamma \ll k_B T$



Can be fit like previous paper

$$\Delta S_{\text{fit}} = (1.02 \pm 0.01) k_B \ln(2)$$

Strong coupling to reservoir
 $\Gamma \gg k_B T$



~~$\Delta S_{\text{fit}} > 10 k_B \ln(2)$~~

(Two temperature regimes for Anderson impurity model?)

Experimental implementation

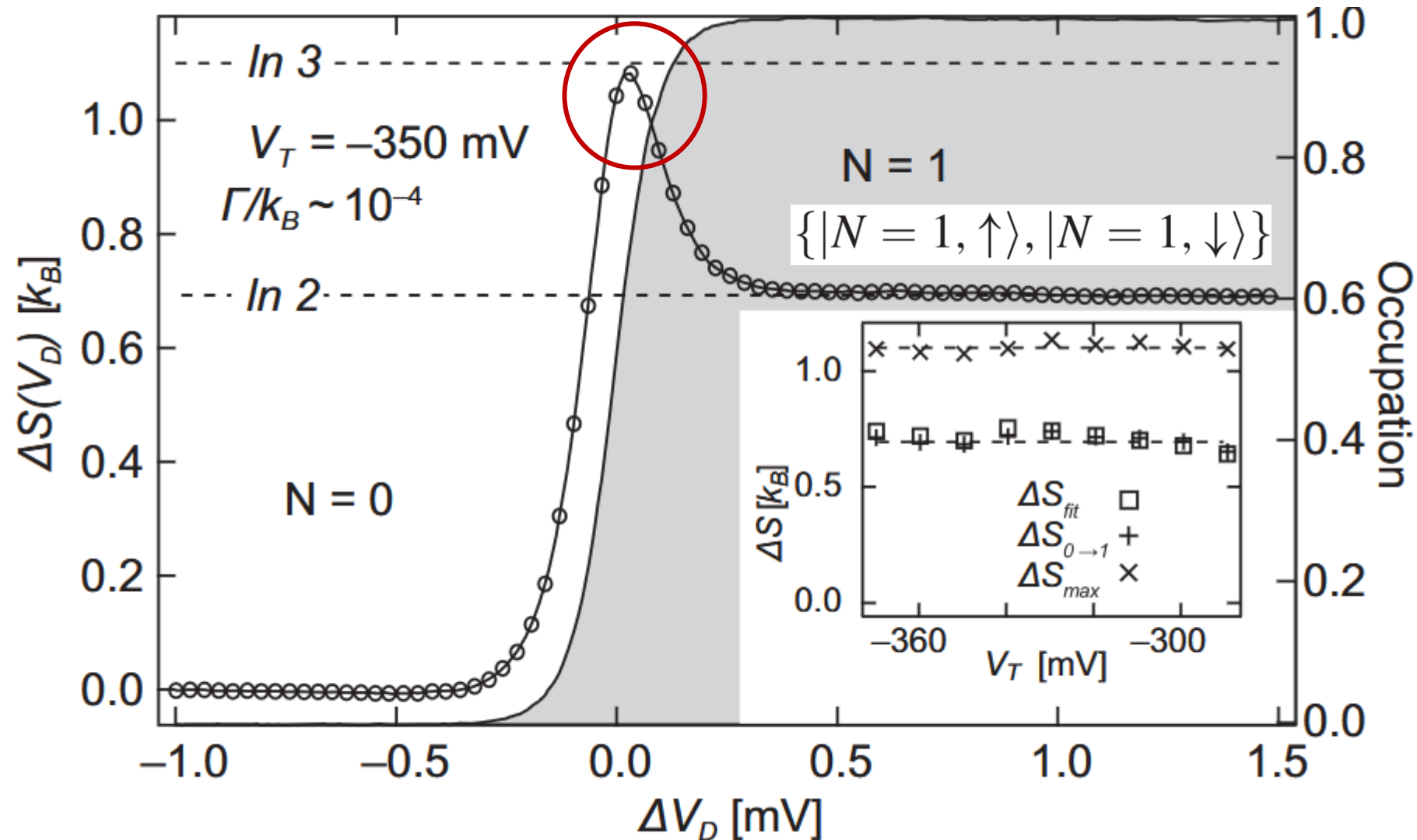
$$\Delta S_{\epsilon_1 \rightarrow \epsilon_2} = - \int_{\epsilon_1}^{\epsilon_2} \frac{dN(\epsilon)}{dT} d\epsilon$$

$$\begin{aligned} dN(\epsilon)/dT &\approx \Delta N(V_D)/\Delta T \\ &\approx -\Delta I_{CS}(V_D)/(I_e \Delta T) \end{aligned}$$

Verification of new technique in weakly coupled regime

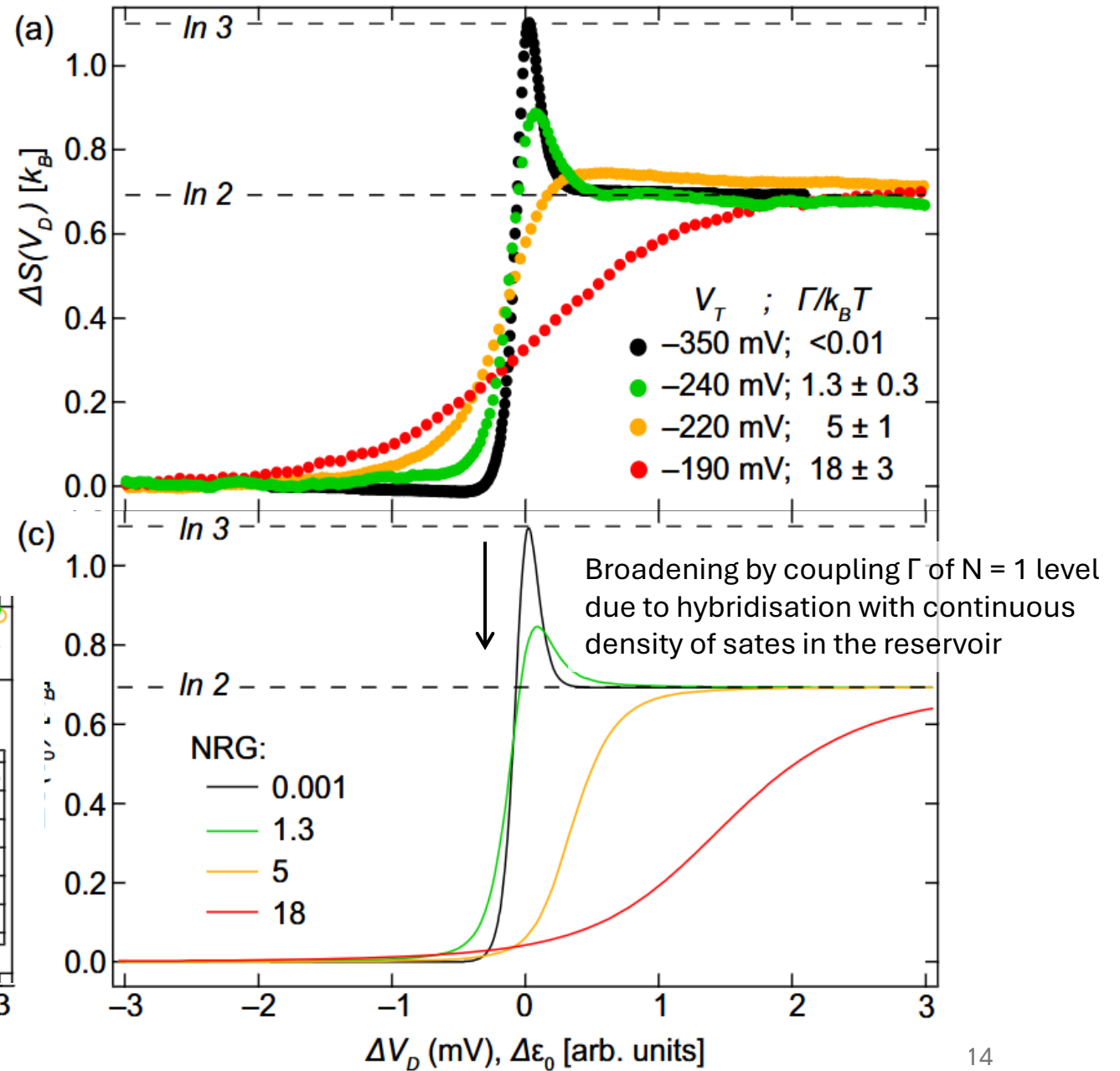
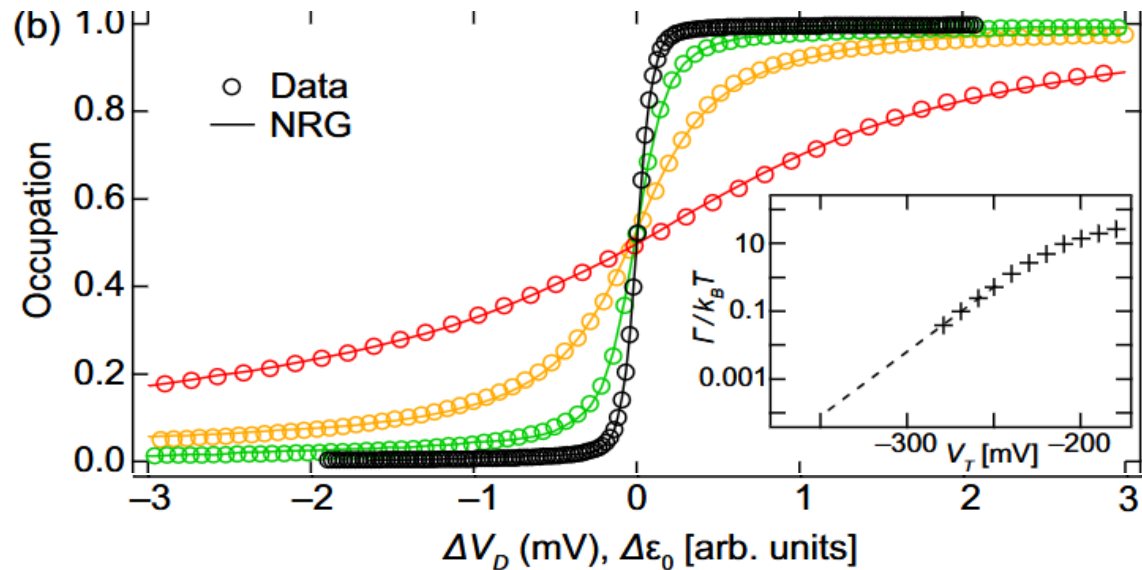
$\Delta S = k_B \ln(3)$: three equiprobable macrostates

$$\{|N = 0\rangle, |N = 1, \uparrow\rangle, |N = 1, \downarrow\rangle\}$$



Transition from weakly coupled to strongly coupled regime

NRG = numerical renormalisation group



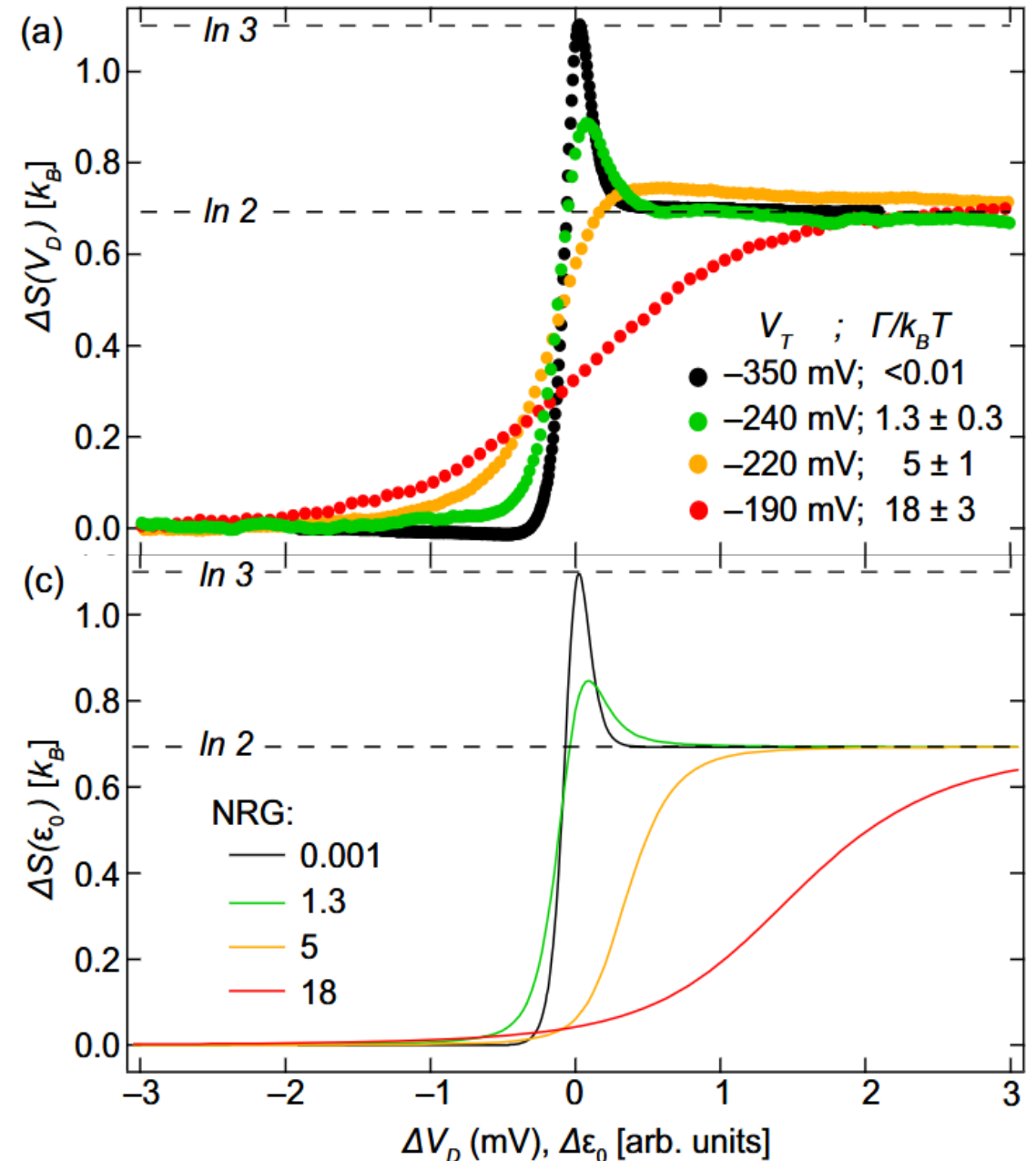
Paper 2

Kondo effect: quasibound singlet state between the localized spin and a cloud of delocalized spins in the reservoir at temperatures below T_K

No magnetic moment and zero entropy for a single-electron QD, so the measured entropy should remain zero for $T < T_K(\epsilon_0)$

However, this is not observed in experimental data.

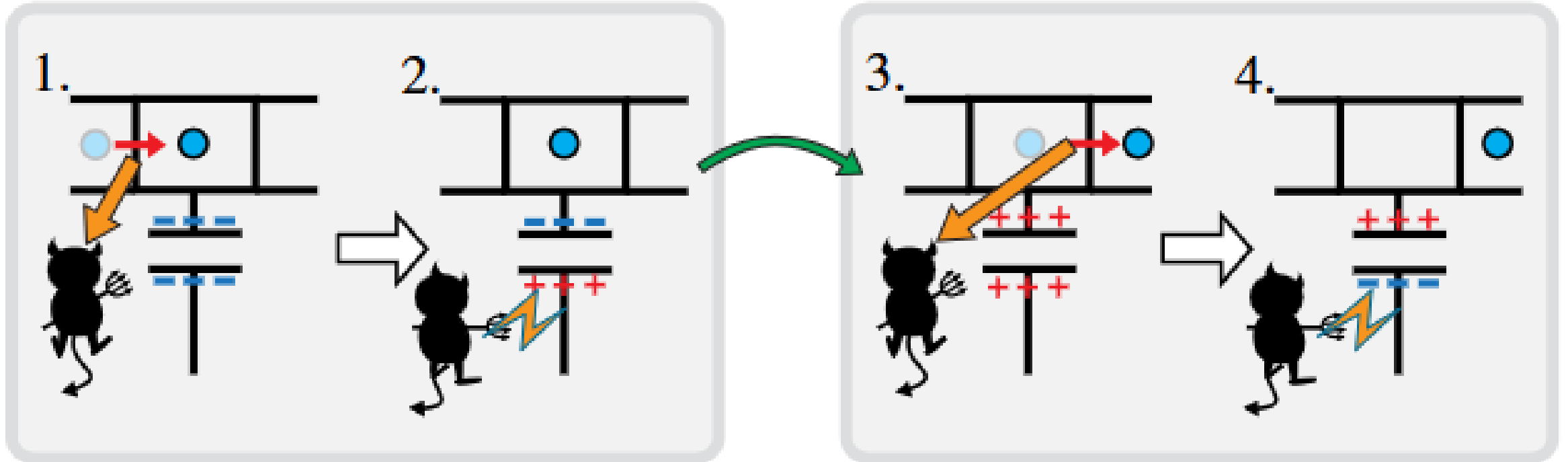
Charge measurements are dephasing the Kondo singlet? At least no dependence observed when changing the charge sensor bias from 300 μ V to 50 μ V.



Conclusion and outlook

- Measurement of quantum dot entropy from charge sensor using temperature dependence of charge sensor reading (in both DC or AC)
- Entropy changes in $k_B \ln(i)$ where i is an integer show the discrete changes in the number of accessible microstates
- Latest approach works even for strong coupling to the environment
- Expected Kondo physics is not showing up in the measurements, what could be the reason?
- To what other systems could this kind of entropy measurement be applied?

Extra: *On-Chip Maxwell's Demon as an Information-Powered Refrigerator*, J. V. Koski et al. (2015)



Entropy move from system to demon, cooling (?) the SET

LACK OF DEPENDENCE ON CHARGE SENSOR BIAS

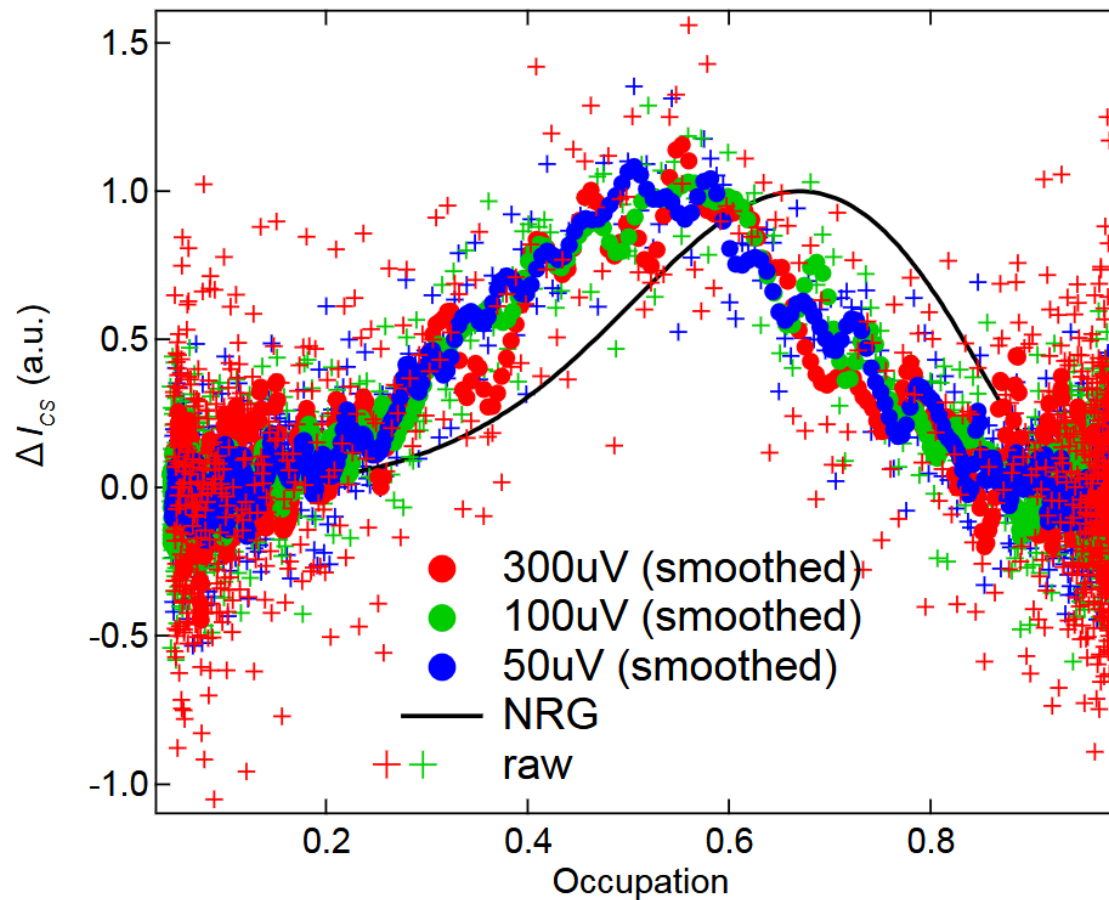


FIG. S5. The lineshape of ΔI_{CS} , here plotted vs occupation instead of V_D , shows no dependence on V_{CS} within experimental noise, though of course the magnitude of I_{CS} and ΔI_{CS} scales linearly with V_{CS} . The case of $\Gamma/k_B T = 24$ is shown here. In particular, ΔI_{CS} remains peaked at $N \sim 0.5$, in contrast to the NRG calculation (solid line) in which the shifted peak reflects the screening of spin entropy in the mixed valence regime due to the formation of the Kondo singlet.

SCALING FROM ΔI_{CS} TO dN/dT

The complete procedure for scaling from ΔI_{CS} to dN/dT is comprised of two parts: Conversion of ΔI_{CS} to ΔN , and calculation of the corresponding ΔT , expressed in equivalent mV on V_D .

The procedure for scaling the ΔI_{CS} measurements to dN/dT involves scaling $\Delta I_{CS} \rightarrow \Delta N$, then dividing by ΔT as described in the main text. The $\Delta I_{CS} \rightarrow \Delta N$ conversion is a straightforward division by I_e (Fig. S3), the net change of current through the charge sensor for the addition of 1 full electron to the QD. In order to extract I_e from the data, measurements of I_{CS} are fit to NRG calculations of dot occupation across the transition, after adding a fixed offset that account for the setting of the charge sensor in the middle of its first charge step, and a linear term that accounts for cross capacitance between V_D and the charge sensor. Examples of the fixed and linear terms are seen clearly in Fig. S1a, where a very wide scan of V_P (over a much larger range than required for the charge transition) is able to completely pinch off the charge sensor, or to bring it to the first plateau. The cross capacitive effect of V_D is much smaller than that of V_P : its lever arm to the QD energy level is much larger, so much only mV or sub-mV changes are required in V_D to sweep across a charge transition.

ΔT is easily extracted in units of equivalent gate voltage (V_D) for weakly coupled V_T by fitting cold and hot occupation data to NRG. For strongly coupled transitions, however, ΔT does not result in a broadening of the transition lineshape, so it must be determined in another way. The real temperature change of the reservoir does not depend on V_T , of course, but the lever arm α does depend on V_T . We calculate $\Delta T(V_T)$ in equivalent mV on V_D by

1. fitting hot and cold transitions for a range of weakly coupled V_T , to determine both $\Delta T(V_T)$ in equivalent V_D and $\alpha(V_T)$ through this range.
2. $\alpha(V_T)$ is observed to be linear in V_T , and extrapolated to strongly-coupled V_T (dashed line in Fig. 1c, main text).
3. ΔT in equivalent V_D is calculated for strongly coupled transitions using $\alpha(V_T)$ determined above.

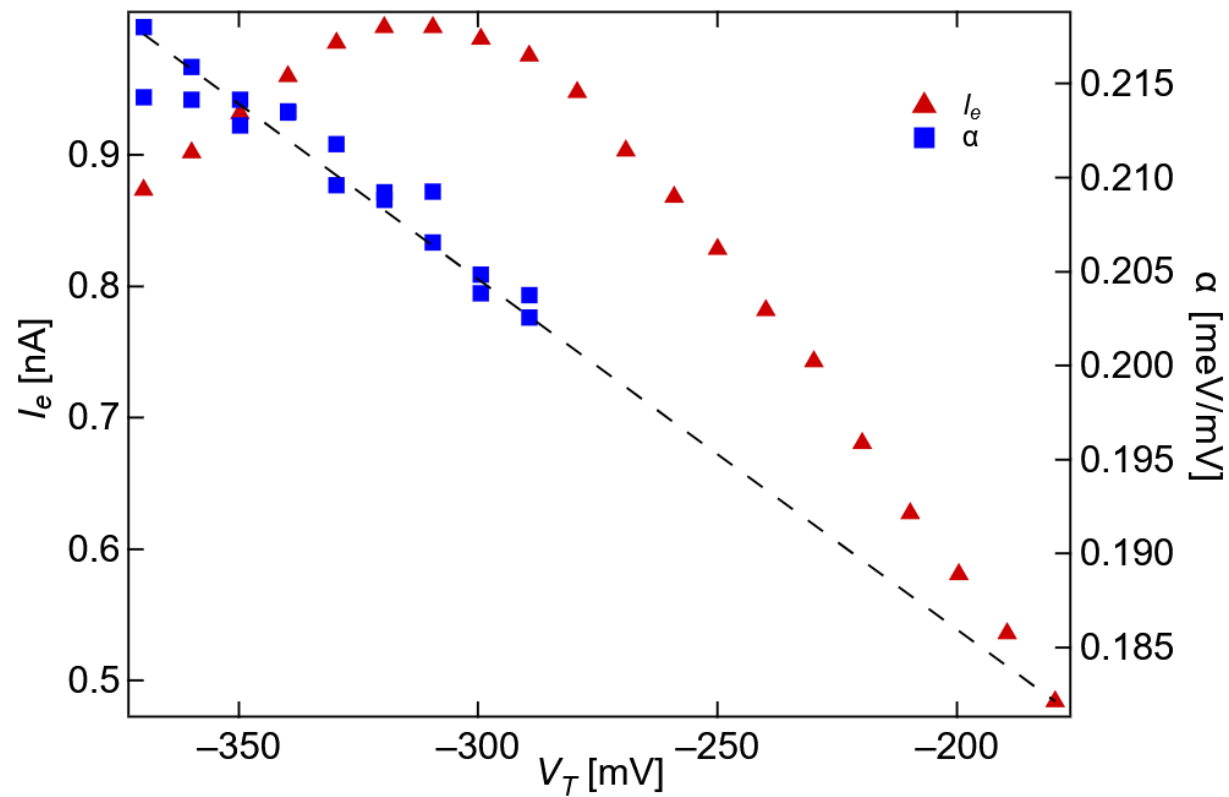


FIG. S3. Variation of lever arm α , and charge step I_e measured independently over the full range of V_T explored in this experiment. Dashed line: extrapolation of α into the strongly-coupled regime where it cannot be measured directly.

Methods

The device was built on a AlGaAs/GaAs heterostructure, hosting a 2DEG with density and mobility at 300 mK of $2.42 \times 10^{11} \text{ cm}^{-2}$ and $2.56 \times 10^6 \text{ cm}^2/(\text{Vs})$ respectively, determined in a separate measurement. Mesas and NiAuGe ohmic contacts to the 2DEG were defined by standard photolithography techniques, followed by atomic layer deposition of 10 nm HfO_2 to improve the gating stability in the device. Fine gate structures, shown in Fig. 1a, were defined by electron beam lithography and deposition of 3 nm Ti/18 nm Au.

The measurement was carried out in a dilution refrigerator with a two-axis magnet. The 2DEG was aligned parallel to the main axis with the second axis used to compensate for sample misalignment. In practice, out-of-plane fields up to 100 mT showed no effect on our data. A retuning of the quantum dot gates was necessary to capture the bias spectroscopy data in Figs. 3d,e and 4e,f. The rightmost gate (Fig. 1a) on the quantum dot was used to tune between the one- and two-lead configurations, for the entropy and bias spectroscopy measurements, respectively. This tuning had a significant effect on the shape of the potential well, accounting for variations in parameters such as g and Δ_{ST} between the two measurement configurations. Charge sensor conductance was measured using a d.c. voltage bias of 200–350 μV ; we find that Joule heating through the sensor does not affect our reservoir temperatures up to $V_{\text{sens}} \sim 500 \mu\text{V}$. The d.c. current (I_{sens}) was measured using an analogue–digital convertor while the a.c. current (δI_{sens}) was measured using a lock-in amplifier. The d.c. conductance reported here is $G_{\text{sens}} = I_{\text{sens}}/V_{\text{sens}}$ while the oscillations are defined as $\delta G_{\text{sens}} = (\delta I_{\text{sens}})/V_{\text{sens}}$.

The temperature of the reservoir was raised above the substrate temperature using I_{heat} at a.c. or d.c., with the QPC heater set by gate voltages to 20 k Ω . Applying a.c. current at $f_{\text{heat}} = 48.7$ Hz yields an oscillating Joule power, $P_{\text{heat}} = I_{\text{heat}}^2 R_{\text{QPC}}$. To leading order, this gives oscillations in temperature, and therefore δG_{sens} , at $2f_{\text{heat}}$. These are captured by the lock-in amplifier at the second harmonic of I_{heat} . Except where noted, measurements of ΔS were made at $\delta T \sim 50$ mK, although the error bars in Fig. 2 demonstrate that the measurements would have been just as accurate with δT set to 30 mK.

We conclude with a few notes to encourage the application of this entropy measurement protocol to other mesoscopic systems. The crucial ingredients in achieving the high accuracy reported here were: the ability to oscillate temperature rapidly enough to avoid $1/f$ noise; the ability to measure charging transitions without perturbing the localized states; and the fact that the charging transitions were thermally broadened. The last criterion enabled the entropy determination purely by asymmetry, without the need to know δT or other measurement parameters accurately, yielding an uncertainty of less than 5%. With this level of precision, it should be possible, for example, to distinguish the $\frac{1}{2}k_{\text{B}} \ln 2$ entropy of a non-Abelian Majorana bound state from the $k_{\text{B}} \ln 2$ entropy of an Andreev bound state at an accidental degeneracy^{11,12}. Similarly, the $S = \frac{1}{2}k_{\text{B}} \ln 2$ two-channel Kondo state could be clearly distinguished from fully screened ($S = 0$) or unscreened ($S = k_{\text{B}} \ln 2$) spin states¹³.

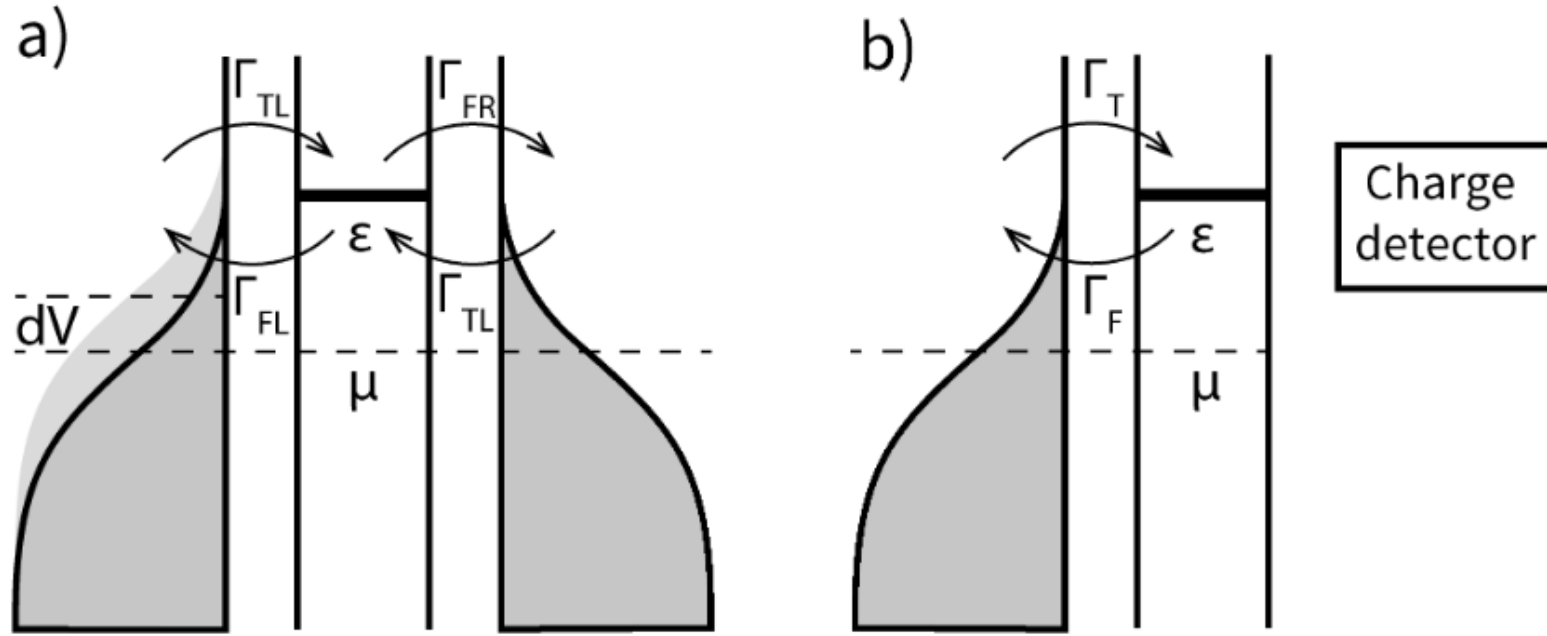


Figure 1. Experimental regimes of Coulomb-blocked nanodevices: (a) A quantum dot coupled to a thermal bath and exchanging electrons with it. The charge state of the quantum dot can be independently determined. (b) A quantum dot coupled to two electrodes through tunnel junctions. A potential difference dV between them can be applied and current through the quantum dot is measured.